Discrepancy between modelled and measured radial electric fields in the scrape-off layer of divertor tokamaks: a challenge for 2D fluid codes ?

A.V. Chankin[1], D.P.Coster[1], N.Asakura[2], X.Bonnin[3], G.D.Conway[1], G.Corrigan[4], S.K.Erents[4], W.Fundamenski[4], J.Horacek[5], A.Kallenbach[1], M.Kaufmann[1], C.Konz[1], K.Lackner[1], H. W. Müller[1], J.Neuhauser[1], R.A.Pitts[6], M.Wischmeier[1]

[1] *Max-Planck-Institut für Plasmaphysik, EURATOM Association, D-85748 Garching, Germany*
[2] *Japan Atomic Energy Agency (JAEA); Naka Fusion Research Institute, 801-1 Mukouyama, Naka-Machi, Ibaraki-ken, 311-0193, Japan*
[3] *CNRS-LIMHP, Université Paris 13 99 AvenueJ.-B. Clément, F-93430 Villetaneuse, France*
[4] *EURATOM-UKAEA Fusion Association, Culham Science Centre, Abingdon, Oxfordshire, OX14 3DB, UK*
[5] *Institute of Plasma Physics, Za Slovankou 3, 182 00, Prague 8, Czech Republic*
[6] *Centre de Recherches en Physique des plasmas, Association EURATOM-Confédération Suisse, École Polytechnique Fédérale de Lausanne, Ch-1015, Switzerland*

Abstract

Examination of radial electric field (E_r) profiles in the scrape-off layer (SOL) of ASDEX Upgrade (AUG) and JET revealed large discrepancies between 2D fluid edge modelling and experiment. Experimental profiles of plasma potential (V_p) in the outer (low field) side of the plasma, obtained with reciprocating Langmuir probes, decay radially with electron temperature, T_e, with the $-eE_r/\nabla T_e$ ratio being > 1.5. In contrast, code simulated E_r are fairly low in most of the SOL (compared to $-\nabla T_e/e$). Modelling with kinetic treatment of neutrals and drifts was performed using the SOLPS code for AUG cases and EDGE2D-Nimbus for JET cases.

Mismatches between modelled and experimental E_r may be caused by the recently established tendency for the SOLPS code to underestimate T_e in the divertor of AUG. It was attributed to non-locality of parallel transport of supra-thermal, heat-carrying electrons originating upstream of the divertor, which are usually only weakly collisional and can penetrate, with few collisions, to the target. Ratios $-eE_r/\nabla T_e$ obtained from the probe measurements in JET are of order 1.6, while in AUG, JT-60U and TCV they are of order 3. Such high values point to the possibility of fast electrons contributing, apart from target heat fluxes, also to the formation of the Debye sheath.

The problem of the underestimation of E_r in the codes must be closely related with the well-known problem of the underestimation of those parts of parallel ion flows in the SOL that are influenced by the toroidal field direction. It was demonstrated earlier that parallel ion flow at the outer midplane is dominated by the ion Pfirsch-Schlüter flow, which in turn is partly driven by the radial electric field. The T_e and E_r discrepancies, as well as discrepancies between simulated and experimental parallel ion flows, put into question the validity of fluid codes for the plasma edge modelling and prompt the inclusion of kinetic effects into present-day 2D fluid codes which assume strong collisionality.

1. Introduction

Recent detailed comparison between ASDEX Upgrade (AUG) experimental data and results of the SOLPS code simulations revealed the tendency for the code solutions to underestimate the target electron temperature and overestimate its density [1,2]. Sensitivity studies of the SOLPS solutions to various assumptions in both plasma and neutral models have almost entirely eliminated the possibility of inappropriate description of neutrals or ions as the cause of discrepancies between the code and experiment [1-3]. The discrepancies are likely to be attributed to supra-thermal electrons in the main SOL plasma (upstream of the divertor, along the field lines). Both Braginskii method of expansion in a small ratio of Coulomb collisional mean-free path λ to the parallel plasma parameter variation scale length L [4] and full kinetic Fokker-Planck modelling for small λ/L ratios [5] predict that most of the parallel plasma heat conduction is carried by supra-thermal electrons. The velocities of such electrons are in the range of 3-5 of electron thermal velocity $v_{T_e} = \sqrt{T_e / m_e}$ (see [5,6], also [7], p.658), with the peak of the heat flux density in velocity space $v_{\|} v^2 f_e$ (f_e being the electron distribution function) located at electron kinetic energies $E_e \equiv m_e v^2 / 2$ close to $6T_e$. Half of the total heat flux is carried by electrons with $E_e \geq 7T_e$ [5]. Such electrons can reach the target after only a few collisions and directly influence target plasma temperature, density and heat deposition profiles. They also raise the Debye sheath potential [5].

An increase in the potential drop at the target surface within the Debye sheath and magnetic pre-sheath (MPS) layers contributes to the build-up of the radial electric field, E_r, in the SOL. Since the largest discrepancies between SOLPS and the experimental target profiles were found for positions near the separatrix [1,2], one may expect the largest deviations between simulated and experimental E_r profiles in the SOL also to occur closer to the separatrix position. This expectation is confirmed by the comparison between simulated and experimental E_r profiles based on a number of SOLPS (B2.5-Eirene) and EDGE2D-Nimbus cases modelling AUG and JET plasmas, respectively, on the one hand, and experimental data from AUG, JET, JT-60U, TCV, on the other, presented in this paper.

In addition to discrepancies between simulated and experimental target T_e and SOL E_r profiles, there exists a long-standing issue of large discrepancies between modelled and measured Mach values of parallel ion flow in the SOL. 'Hotter' SOLPS solutions for the divertor, with higher target T_e, were found to predict larger Mach numbers and larger E_r [8,3]. It was suggested in the latter ref. that the discrepancies in target T_e and Mach numbers can be related to each other, with the link between them being provided by the radial electric field in the SOL. Following [3], experimental confirmation for the existence of large E_r in the SOL was obtained and numerical estimates for the relation between the E_r and predicted parallel ion flows by SOLPS and EDGE2D were made. They lead to the conclusion that the correct, experimentally determined E_r profiles in the SOL would indeed largely eliminate severe mismatches between field-dependent (dependent on the toroidal field direction, in single-null divertor configurations) modelled and experimental Mach numbers of the parallel ion flow in both AUG and JET [9].

This paper is organized as follows. Results of modelling E_r in the SOL with the two widely used 2D fluid codes: SOLPS and EDGE2D-Nimbus, are presented in Section 2. They are followed by the results of the Lagmuir probe and Doppler reflectometer measurements of E_r in AUG described in Section 3, and the results of probe measurements in JET - in Section 4.

Additional supporting experimental evidence from JT-60U and TCV is provided in Section 5. Implication of the discrepancies between modelled and experimental E_r values, as well as high E_r values observed in some experiments, are discussed in Section 6. The work is summarised in Section 7.

2. Modelling E_r with SOLPS and EDGE2D

The AUG and JET plasmas selected for the 2D edge modelling described here cover various conditions, primarily with respect to n_e and T_e values in the SOL and divertor. SOLPS cases were run with the coupled fluid plasma part, B2.5, and a kinetic Monte-Carlo neutral solver, Eirene. Similarly, EDGE2D was coupled with the neutral Monte-Carlo code Nimbus. Drift terms were fully switched on across the whole numerical mesh in the EDGE2D code. In B2.5, they were switched on across SOL, private region and about 1/3 of the core region adjacent to the separatrix. For both SOLPS and EDGE2D results presented below, T_e and plasma electric potential V_p profiles across the SOL are plotted against distance from the separatrix at the outer midplane position.

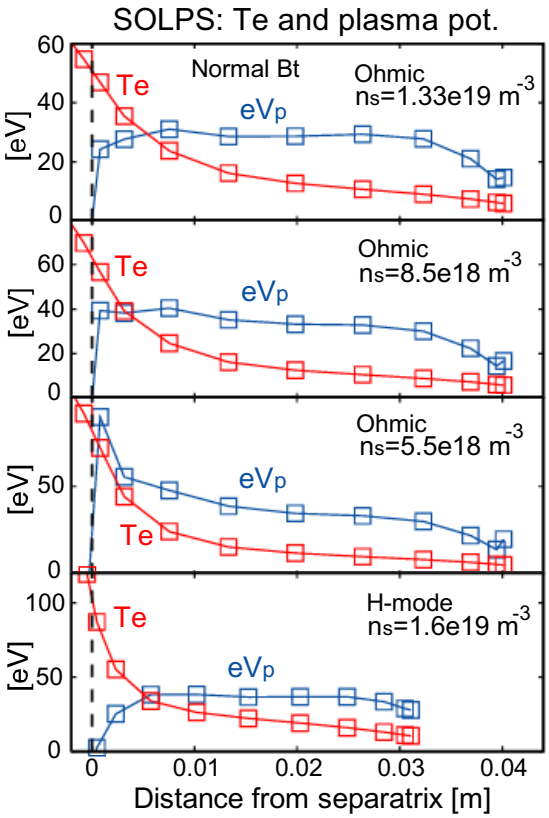

Fig. 1. Outer midplane profiles of electron temperature and plasma potential from SOLPS cases modelling AUG plasmas with normal Bt direction. Anomalous conductivity must have affected the H-mode case (see text for details).

The Ohmic SOLPS outer midplane profiles presented in Fig. 1 are based on the previously modelled standard AUG Ohmic case with medium density described in [10] (with fluid neutrals) and [2] (with Monte-Carlo neutrals). The normal Bt case (with the toroidal field Bt directed such that the ion ∇B drift is towards the X-point) analysed there matches very well experimental upstream (obtained near the outer midplane position) n_e and T_e profiles, with somewhat poorer match to the T_i profile. It was not possible to match the divertor parameters in those calculations: the simulated outer target T_e in the cases with Monte-Carlo neutrals was too low, and n_e too high, compared to the experiment, and the radiated power (on deuterium only) slightly exceeded its experimental value, despite chemical sputtering being switched off, leading to almost complete elimination of impurities. Problems with matching target profiles are likely to be related with endemic deficiencies of the fluid codes in treating high energy electrons that are responsible for the bulk of the parallel heat flux. The AUG standard Ohmic case is quite representative of plasma edge conditions in this machine regarding collisionality. As was pointed out in [2], it also has the same midplane separatrix electron dimensionless collisionality (see the definition of it given by Eq. (1)) as that expected in ITER [11].

In the present study, two more cases, at lower electron separatrix densities n_s, were run, in order to cover possible regimes with 'hotter' (higher T_e) plasmas in the divertor. These simulated plasmas have no experimental equivalents. In addition, data for the low density H-mode shot in the normal Bt configuration, analysed earlier in [1], are also presented in Fig. 1.

SOLPS cases presented in Fig. 1 had small anomalous radial currents related to E_r and ∇T_e (the latter – only for the H-mode case). The anomalous conductivity is controlled by the parameter *fsig*, and anomalous thermo-electric current – by *falf*. The electrical conductivity and thermo-electric coefficients are given by $fsig \times 1.6 \times 10^{-19} n_e(m^{-3})$ and $falf \times n_e(m^{-3}) T_e(eV)^{-1/2}$ is MKS units, respectively. The default values for both parameters in SOLPS are 1×10^{-3}. These anomalous currents were introduced into SOLPS for the sake of improving numerical stability of the code. For Ohmic cases shown in Fig. 1, *fsig* was reduced to 1×10^{-4} and *falf* was set to zero. Such a change in the coefficients, compared to the cases with the default settings, was found to mainly influence (increase) electric potential on the first ring outside of the separatrix, while in the rest of the SOL E_r was little affected. Further reduction in *fsig* didn't result in any appreciable changes in the potential profile, but detrimentally affected stability of the code runs. For the H-mode case, the default values for *fsig* and *falf* were used, for the sake of numerical stability. All reversed field cases (with the toroidal field Bt directed such that the ion ∇B drift is away from the X-point), not shown in Fig. 1, also required default settings of these parameters.

As one can see from Fig. 1, for the highest density Ohmic and H-mode cases, plasma potential rises from the separatrix deeper into the SOL up to a distance of $\approx$ 0.5 - 1 cm, then is stabilizes, and finally drops further out, at distances larger than 3 cm. Too low, almost zero, potential on first ring outside of the separatrix in the H-mode case is an artifact related to anomalous radial currents introduced into SOLPS, as pointed out earlier. In the most of the SOL, E_r is almost zero for H-mode and the highest density Ohmic cases. For the Ohmic cases with reduced separatrix density of 8.5×10^{-18} m^{-3}, E_r values obtained from the code were small, well below $-0.5\nabla T_e/e$, across most of the SOL. They only showed an increase in the far SOL, at the position of $\approx$ 3.25 cm from the separatrix, where the plasma density is already too small. The only case that had appreciable E_r values across most of the SOL was the Ohmic case with extremely low $n_s = 5.5 \times 10^{18}$ m^{-3}. The $-eE_r/\nabla T_e$ ratio reached $\approx$ 1 near the separatrix in this case. The main reason for the $-eE_r/\nabla T_e$ increase at low densities is the peaking of target T_e profiles. This results in the peaking of the target Debye sheath potential profiles that raises the upstream E_r (see Sec. 6).

The selected EDGE2D cases for Ohmic JET shots repeat those previously modelled and described in [12]: #56723 for normal, and #59737 – for reversed Bt cases (note different meshes in Fig. 2). Two density phases of these shots, referred to as having 'high' and 'low' separatrix density n_s, were modelled in [12] by varying the amount of the gas puff in the modelling. Contrary to SOLPS cases, which were severely constrained by having to match extremely good quality upstream profiles, and consequently having problems with matching target profiles, the latter were given much more weight in specifying input parameters for EDGE2D runs. Experimental target profiles, mainly of the n_e and T_e, obtained by Langmuir probes, were fairly well matched in the EDGE2D modelling.

In the original EDGE2D cases described in [12], drifts were switched on only in the SOL, but switched off in the core, owing to numerical instabilities originating in the core region.

Recent improvements in the code have enabled switching drifts on everywhere in the grid. In the present simulations, these cases were run further with drifts switched on everywhere up to the new steady-state, which however showed only insignificant deviations in midplane T_e and V_p profiles in the SOL, as well as in the target parameters, from the original cases. However, Mach numbers of the ion parallel flow were somewhat higher. Similar to SOLPS, small radial anomalous conductivity is used in EDGE2D cases, but only in the core region. In contrast to SOLPS, there are no anomalous currents in the SOL and divertor regions.

The EDGE2D H-mode case with normal Bt was modelled in [13]. It corresponds to JET Type-I ELMy H-mode discharge with NBI input power of 12 MW, Bt = 2.4 T and Ip = 2.5 MA. Drifts were switched on in these calculations. In the present paper, the same case was continued with the reversed field direction until it reached steady-state.

The main signatures of the V_p profiles shown in Fig. 2 repeat those of the SOLPS cases. Some difference between the normal and reversed field V_p profiles for low density Ohmic cases may be caused by lower, by ≈ 10%, density in reversed Bt case, which also gives rise to higher separatrix T_e. (The same difference between high density Ohmic cases, however, doesn't result in any appreciable difference in V_p profiles). Similarly to SOLPS cases, the V_p profiles across most of the SOL show almost no resemblance to the T_e profiles. Steepening of V_p profiles for low density cases is mainly caused by peaking of target T_e profiles, similar to SOLPS cases.

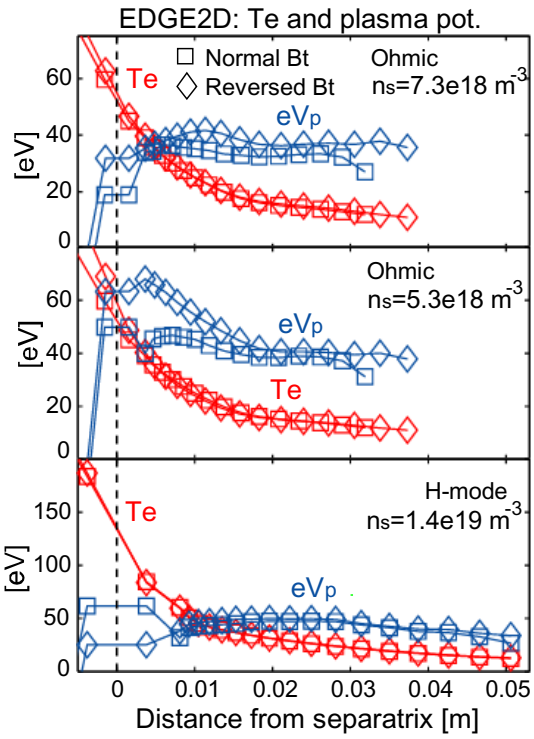

Fig. 2. Outer midplane profiles of electron temperature and plasma potential from EDGE2D cases modelling JET plasmas.

Since kinetic effects in the parallel electron transport have been invoked earlier in order to explain the discrepancy between measured and simulated parameters in the divertor of AUG, it is useful to introduce the dimensionless electron collisionality upstream, close to the outer midplane. For a rough estimate, it can be defined, following [7] (p.194, Eq. (4.105)) as:

$$\nu^*_{ee} = 10^{-16}\,\frac{n_e(m^{-3})\pi q_{95} R(m)}{T_e(eV)^2}, \qquad (1)$$

where the connection length L was replaced by $\pi q_{95} R$, with q_{95} being the safety value at the 95% poloidal flux surface. This collisionality, calculated for separatrix n_e and T_e values, will be used to compare different code runs and different experiments/plasmas. For SOLPS cases shown in Fig. 1, collisionalities ν^*_{ee} are (from top to the bottom box): 14.1, 8.4, 6.6 and 3.5. As pointed out earlier, the highest collisionality, corresponding to the standard AUG Ohmic plasma, is very close to the expected collisionality in ITER. For the EDGE2D cases presented in Fig. 2, the collisionalities are (from top to bottom): 7.2, 6.3, 1.1. Together, SOLPS and EDGE2D cases cover a fairly broad range of upstream separatrix collisionalities. These

values will be compared with the estimated collisionalities in the experiments discussed below.

Experimental data on the radial electric field in the SOL presented below by no means represent a thorough review on this subject. A rather limited selection of experimental devices and results of the E_r measurements mainly with Langmuir probes covered in the following sections is only meant to demonstrate the most basic features of the E_r profiles in the SOL. However, even a brief overview of the available probe data from AUG and JET, as well as from JT-60U, TCV and earlier published Alcator C-Mod data, provides a convincing evidence for large discrepancies between measured and modelled (with 2D fluid codes) E_r profiles.

3. Experimental data on E_r from AUG

Reciprocating Langmuir probes, which are typically used to evaluate plasma potential V_p, directly measure floating potential V_f, among other plasma parameters (mainly T_e and the ion saturation current I_{sat}, from which plasma density can be evaluated). Evaluation of the E_r therefore requires knowledge of the difference $(V_p - V_f)$ which is usually taken from theory to be $\sim 3T_e/e$ (see below). In order to provide consistency between various pieces of experimental information supplied by different machines on the evaluated E_r, the most frequently encountered assumption $e(V_p-V_f)/T_e = 3$ will be used throughout this paper. Thus, by differentiating the equation $V_p = V_f + 3T_e/e$ (see e.g. [7], p.520, Sec. 17.3), the radial electric field will be derived as:

$$E_r = -\nabla V_f - 3\nabla T_e / e \qquad (2)$$

from probe measurements of V_f and T_e, where the gradient sign implies gradient over the perpendicular (radial) direction.

Figure 3 shows T_e and V_f data obtained by the reciprocating Mach probe (Langmuir probe capable of measuring Mach number of parallel ion flow) introduced just above the outer midplane, as described in [14,15]. The discharge parameters were: line-average density $\bar{n}_e = 3.65\times10^{19} m^{-3}$, toroidal field Bt = 2 T, plasma current Ip=0.8 MA, $q_{95} = 4$. This is a standard AUG Ohmic shot, with the same parameters as shot #18737 modelled by SOLPS and described in Section 2. The data presented here were obtained by the same pins of the reciprocating probe as those used for measuring parallel ion Mach number. The probes, separated by a partition, were facing outer ('l-values') or inner ('r-values') divertor along the field lines. Owing to a strong parallel ion flow in the direction from the outer to inner divertor at the probe position in this normal Bt discharge, plasma density (ion saturation current was the directly measured signal) was larger at the flow-facing pins ('l-values'), leading also to higher floating potential than for downstream pins, as one can see from Fig. 3. The difference between the V_f values is especially large near the separatrix. Calculated plasma potentials show steep rise towards the separatrix position for both up- and down-stream pins, with the calculated $-eE_r/\nabla T_e$ values obtained as $e\Delta V_f/\Delta T_e$ over the last 1.5 cm of the probe reciprocation being of order 3. This is in a sharp contrast with the modelling results described in Sec. 2, where E_r is nearly zero for most of the SOL (see the V_p profile in the top box of Fig. 1). Due to low T_e values, ≈ 18 eV, measured by the probe even at the closest position to the separatrix, the probe apparently didn't go far into the plasma, stopping at a distance of 0.5

- 1 cm from the separatrix, judging by the value of the separatrix T_e (≈ 45 eV, according to the SOLPS modelling) and the T_e profile measured by the YAG laser.

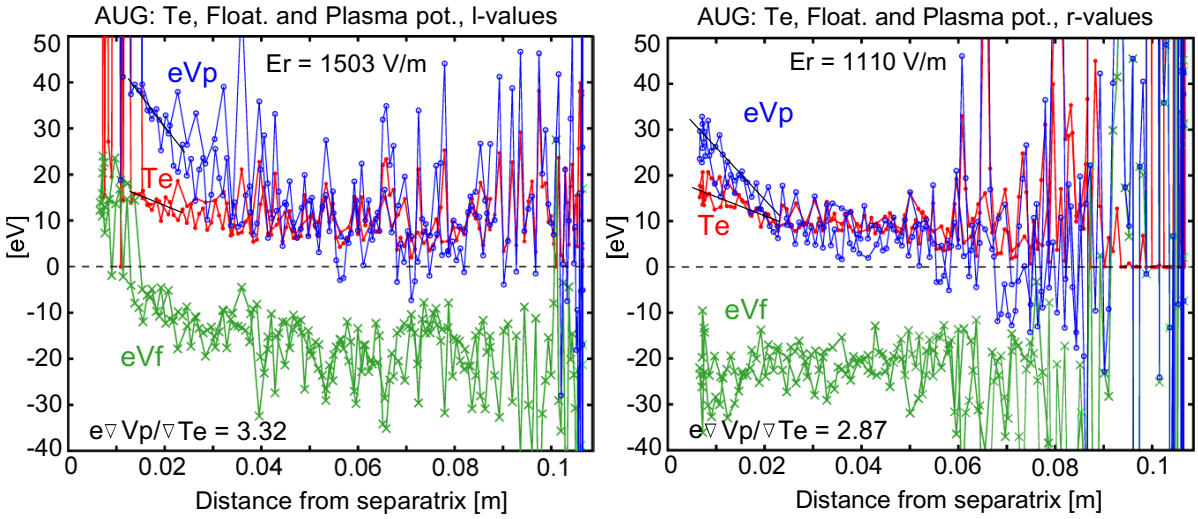

Fig. 3. T_e, floating and plasma potential profiles invoked from the reciprocating Langmuir probe in the standard AUG Ohmic shot. 'l' and 'r'-values refer to data coming from the probes separated by a partition and facing outer and inner divertor along the field lines, respectively. 'Distance from the separatrix' is measured along the probe reciprocation trajectory, which is above the midplane.

The average electron density (between the two probe pins, with the data from the r-pin being linearly extrapolated onto the innermost position of the l-pin) was 1.6×10^{19} m^{-3}. Taking this density, T_e = 18 eV, machine parameters and q_{95} = 4, one obtains for the collisionality defined according to Eq. (1): ν^*_{ee} = 105, which is the highest value of all measured and code simulated cases presented in this paper. Note however, that this collisionality is calculated not at the separatrix position but at a position inside of the scrape-off layer. Also, there are doubts related to the correctness of the determination of electron temperature from the Langmuir probes, since the probe T_e profile is flatter than that obtained from the YAG laser measurements (see below in this section). Related to a possible underestimate of the probe T_e, is the apparent overestimate of its density n_e (1.6×10^{19} m^{-3}) which is higher than the electron separatrix density $n_s = 1.33\times10^{19}$ m^{-3} of the SOLPS solution (see Fig. 1, top box).

An estimate of the E_r in the SOL can also be obtained from Doppler reflectometry. The technique and diagnostic on AUG are described in detail in [16]. By poloidally tilting a microwave reflectometer a Doppler frequency shift is induced in the measured turbulence spectrum $f_D = u_\perp k_\perp/2\pi$ which is directly proportional to the velocity $u_\perp = v_{E\times B} + v_{ph}$ (where v_{ph} is phase velocity) of the turbulence moving in the plasma $E_r\times B$ frame. $k_\perp$ is the measured turbulence wavenumber selected by the tilt and plasma geometry. Linear and non-linear numerical turbulence simulations indicate that turbulence phase velocity v_{ph} is of the order of a few tens to hundreds of m/s at the measured $k_\perp \sim 8$ cm^{-1} [17,18], which is small compared to $v_{E\times B}$ thus allowing E_r to be approximated directly as $u_\perp B$. Although the electron diamagnetic velocity is a factor of 3 or so larger than $u_\perp$ (see below, the combined effect of electron density and temperature gradients measured by the YAG laser in Fig. 4), a $v_{ph} \sim 0$ is not unexpected since linear gyrokinetic simulations on closed field lines indicate that the drives from the comparable density and ion temperature gradient lengths can counteract [19].

Note that the sharp reversal of E_r across the separatrix reflects the strong velocity shear in the pedestal gradient region (see e.g. [16]).

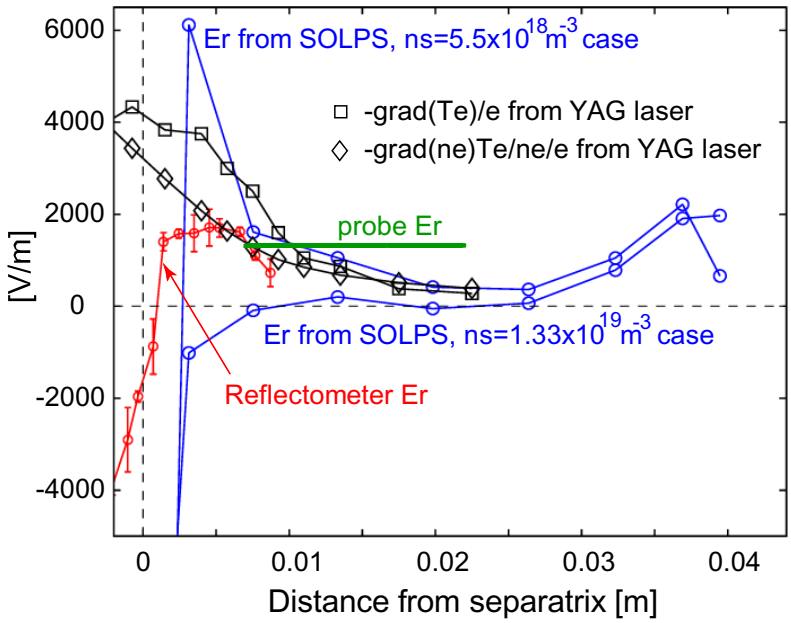

Fig. 4. Experimental and modelled profiles for the Ohmic AUG shot: E_r profile measured by the Doppler reflectometer, $-\nabla T_e / e$ and $-T_e \nabla n_e / n_e e$ profiles from the YAG laser, averaged E_r from the reciprocating Langmuir probe (see original data in Fig. 3), and E_r from Ohmic SOLPS cases with two levels of density (see V_p profiles in Fig. 1).

Fig. 4 shows the measured E_r profile (assuming v_{ph} = 0) for the equivalent Ohmic shot #18813 from inside the separatrix to a few cm into the SOL. The radial extent is determined by the reflectometer probing frequency range and the SOL density profile. Also shown in this figure are $-\nabla T_e/e$ and $- T_e\nabla n_e/n_e e$ profiles obtained from the interpolation of the YAG laser data, averaged E_r obtained from the data shown in Fig. 3 (the data is averaged over the radial distance of 1.5 cm as well as between the two probes), and the simulated E_r from the two Ohmic SOLPS cases for the highest and lowest density using V_p profiles shown in Fig. 1. Outer midplane YAG laser n_e and T_e profiles, as well as the T_i profile measured by the Li beam diagnostic, can be found in [2].

As can be seen from Fig. 4, the Doppler reflectometer E_r is below $-\nabla T_e/e$, in contrast with the ratio $-eE_r/\nabla T_e \sim 3$ following from the probe measurements. There is, on the other hand, no direct conflict with the E_r invoked from the probe. The average probe E_r value, 1307 V/m, is quite close to the reflectometer data, albeit at larger radii. An additional complication with the data for this shot comes from the difference in the gradients of T_e profiles measured by the YAG laser and the Langmuir probe, as pointed out above. The YAG T_e profile is fairly well resolved spatially, and it exhibits sharp flattening of the T_e profile over the distance indicated by the segment labeled 'probe E_r' in Fig. 4. The ∇T_e from YAG changes from being ~ 7 times larger than the averaged probe $-eE_r$ at the innermost probe position (where the probe T_e coincides with the YAG T_e, both equal to ≈ 18 eV; this equality is not coincidental, but was used to determine the absolute probe position with respect to that of YAG chords, as plotted in Fig. 4) to being somewhat smaller than it at the end of the 'probe E_r' segment. Provided one uses the YAG T_e profile, probe floating potential averaged between the two pins and $-3T_e/e$ for the difference between V_f and plasma potential V_p, one obtains high E_r values, ≈ 8000 V/m, at the innermost probe position, and only ≈ 800 V/m for the outermost position of the 'probe E_r' segment.

SOLPS E_r profile for the higher density Ohmic case, that matches experimental upstream profiles shown in Fig. 4, is much below both the reflectometer and Langmuir probe values, except for the outer SOL positions > 3 cm away from the separatrix. It is possible to greatly increase E_r by a large reduction in the separatrix density. Such SOLPS solutions, however, are unrealistic, since their separatrix n_e and T_e values strongly deviate from the relation between these two quantities established from the YAG laser data.

4. Experimental data on E_r from JET

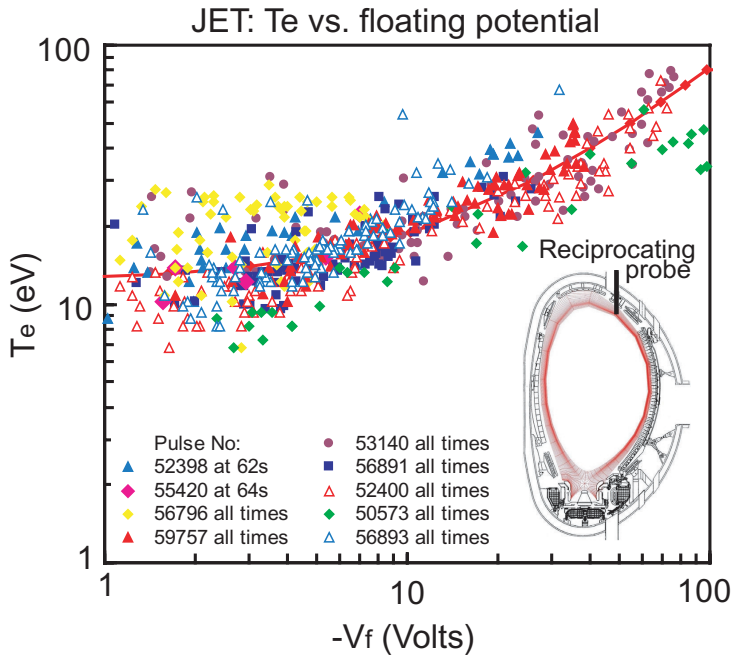

Fig. 5. Relationship between electron temperature T_e and floating potential V_f obtained by the reciprocating Langmuir probe for a number of JET discharges with different confinement properties and taken at different positions during the probe reciprocation. The floating potential is measured with respect to the torus potential The figure is replicated from ref. [12], with minor alterations.

The largest statistical information on the distribution of plasma potential in the SOL was obtained on JET. The results are described in the paper dedicated to comparison between experimental and code simulated parallel ion flows [12]. The reciprocating probe was introduced from the top of the machine, but shifted outward, as indicated in Fig. 5. A number of representative Ohmic, L- and H-mode shots was used to compile the database on the relationship between T_e and V_f, the latter measured with respect to the torus potential (the same as the target potential). The results are shown in Fig. 5. The T_e values were obtained by averaging between the two probe pins facing opposite sides (inner and outer target, along the field lines) of the Mach probe, whereas the V_f data were taken by a separate probe, protruding into the plasma (a small adjustment has been made in Fig. 5 for different positions of T_e and V_f with respect to the plasma position). The dependence of V_f on T_e can be interpolated by the offset linear dependence (in eV): $eV_f = -1.43T_e + 17$, and the best fit to the experimental data is shown by the solid line in Fig. 5. This fit is used here to evaluate plasma potential V_p. A relation between V_f and V_p can be obtained by using a formula given by Stangeby [20]. Combining contributions from the Debye sheath (Eq. (16) of [20]) and magnetic pre-sheath (formula on p.686 of [20]) one obtains:

$$e(V_f - V_p) = 0.5T_e \ln\left[2\pi \frac{m_e}{m_i} \frac{(1+T_i/T_e)}{(1-\delta)^2}\right] - 0.7T_e, \qquad (3)$$

where δ is secondary electron emission. For T_i/T_e = 2, which seems in agreement with experimental data, deuterium plasma and δ= 0.3, one obtains $e(V_f - V_p) = 2.98T_e$, which is in a good agreement with Eq. (2).

Combining Eq. (2) with the best fit for the V_f versus T_e dependence, one obtains: $-eE_r/\nabla T_e$ = 1.57. This ratio can be reduced below 1.57 by increasing secondary emission, with $\delta > 0.3$, or by increasing T_i/T_e ratio, above 2. It can, on the other hand, also be increased if one takes into account the presence of impurities (formulas above assume pure deuterium plasma). The ratio $-eE_r/\nabla T_e$ invoked from the JET data, despite being below that found in AUG, is still in a clear contradiction with the results of the EDGE2D modelling described in the previous section. Experimental trends observed in AUG and JET are confirmed by the data supplied from JT-60U and TCV tokamaks considered next.

5. Supporting experimental evidence from JT-60U and TCV

Reciprocating probe measurements on JT-60U described in this section were performed by a double-sided (Mach) probe introduced from the low field side, 35 cm below the equatorial midplane. Given the size of the machine (R = 3.44 m, a = 0.96 m), the probe position may be regarded as being very close to the outer midplane, similar to the geometry of AUG measurements. The measured V_f and T_e profiles shown in Fig. 6 are for the L-mode shot in

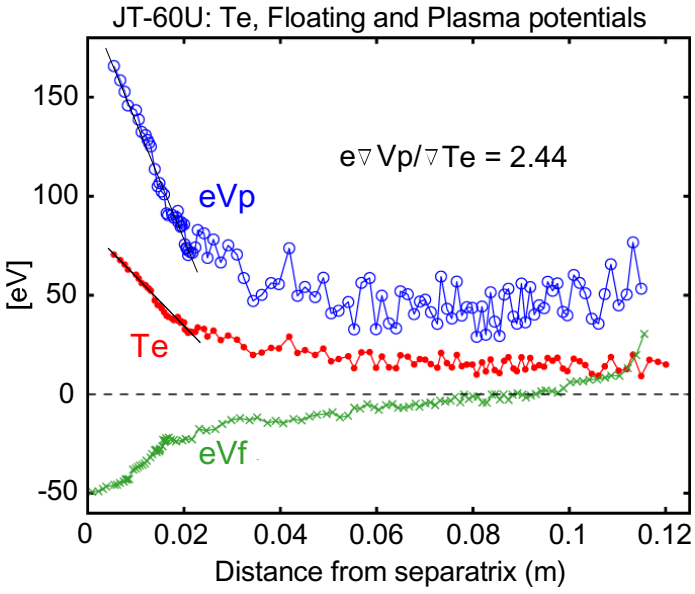

Fig. 6. Te, floating and plasma potentials for the L-mode JT-60U shot measured by the reciprocating Langmuir probe introduced below the outer midplane position. See details in the text.

normal Bt configuration, with Bt = 3.5 T, Ip = 1.7 MA, NBI power of ≈ 4.2 MW and line average density $\bar{n}_e = 1.5\times10^{19}$ m^{-3}. This shot was part of the density scan with $\bar{n}_e$ varying from 1.0 to 3.2×10^{19} m^{-3}, and was selected as representative for the analysis of the nature of parallel ion flows in [21] (see Fig. 5 and related text in this ref., where details of the measurements can also be found). The T_e plotted in the figure is an averaged value of temperatures measured by the two sides of the Mach probe, while the V_f was measured with a separate probe protruding into the plasma and being 4.5 mm closer to the separatrix than the other probes used to measure n_e and T_e. The T_e data in Fig. 6 were correspondingly shifted from the V_f data by this distance. As one can see from this figure, the V_p profile within the

first 2 cm into the SOL is rather steep, with the $-eE_r/\nabla T_e$ ratio being 2.44. The average electron density (between the two probe pins) reached 6.5×10^{18} m^{-3}. Taking this density and the highest T_e (71 eV) measured by the probes, machine parameters and $q_{95} = 3.5$, one obtains for the collisionality defined according to Eq. (1): $\nu^*_{ee} = 4.9$, which is in between collisionalities estimated for the AUG H-mode case and the Ohmic case with $n_s = 5.5\times10^{18}$ m^{-3}.

Langmuir probe measurements in TCV [22] are in good agreement with basic signatures of the V_p profiles observed in AUG and JT-60U. Fig. 7 shows V_p and T_e profiles obtained in this machine for an Ohmic plasma with Bt = 1.43 T, Ip = 260 kA, in reversed Bt configuration. The plasma, which is usually formed in the top half of the vacuum chamber in TCV, was positioned near the centre of the machine in these experiments, so that the reciprocating Mach probe, introduced from the outer (low field) side, as in AUG and JT-60U cases, could reach the separatrix. Similar T_e but slightly different V_f profiles were obtained for the three positions of the plasma, with the axis of the magnetic configuration coinciding with the equatorial plane of the vacuum chamber (in which case the probe movement was exactly within the midplane; Z=0 cm, the case shown in Fig. 7), as well as slightly upward (Z = +10 cm) and downward (Z = -10 cm) shifted plasmas. The three pins of the probe, used to measure T_e, n_e and V_f, were protruding into the plasma and on the same magnetic flux surface.

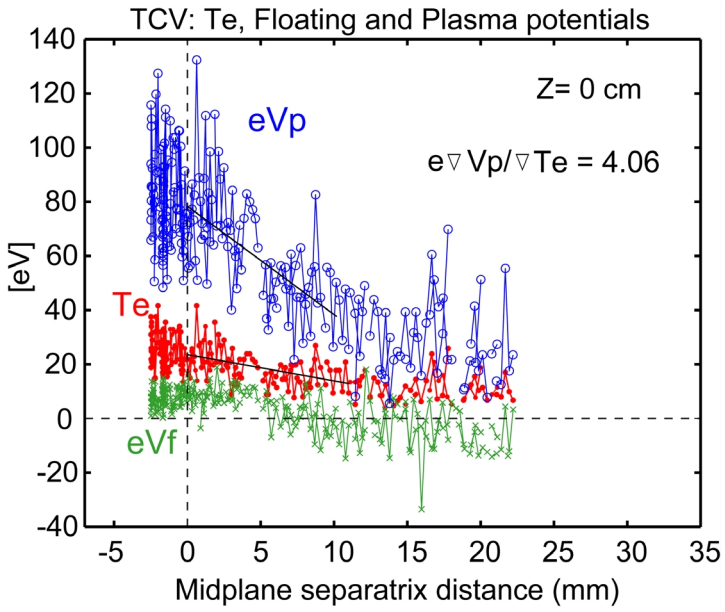

Fig. 7. Te, floating and plasma potentials for the Ohmic TCV shot measured by the reciprocating Langmuir probe introduced along the outer midplane. See details in the text.

As one can see from Fig. 7, the $-eE_r/\nabla T_e$ ratio in TCV for this configuration, using probe positions within 1 cm from the separatrix, is even larger than in AUG and JT-60U plasmas, being ≈ 4 (for Z = +10 cm configuration this ratio was 3.27, and for Z = -10 cm – 4.97). The line-averaged plasma density was $\bar{n}_e = 4.2\times10^{19}$ m^{-3}, in the middle of the density range, from 1.7 to 7.3×10^{19} m^{-3}, in this series of discharges aimed mainly at measuring Mach numbers of the parallel ion flow. Using measured separatrix parameters: $n_s = 1.4\times10^{19}$ m^{-3}, $T_e = 25$ eV, the machine parameter R = 0.87 m (a = 0.25 cm for these plasmas) and the safety value $q_{95} = 3.5$, one obtains for the dimensionless collisionality at the separatrix: $\nu^*_{ee} = 21.6$, which is the

second highest value (after the AUG collisionality, calculated for a position outside of the separatrix) of all measured and code simulated cases presented in this paper. It has to be noted, however, that the TCV tokamak has highly unconventional divertor geometry with a very long outer divertor leg. Estimates show that this should increase the effective dimensionless collisionality by more than a factor of 2.

6. Discussion

Comparison between measured and simulated radial electric fields in the SOL reveals a clear gap between experimental and modelled E_r values, despite both experimental and modelled plasmas covered wide and overlapping range of experimental conditions with respect to the dimensionless separatrix collisionalitiy. The $-eE_r/\nabla T_e$ ratios at the outer midplane in the code simulations are typically well below 0.5. In contrast, in all experimental Langmuir probe profiles presented in this paper, as well as statistical results from JET, this ratio is above 1.5. Earlier experimental evidence from Alcator C-Mod [23] also suggests large and positive $-eE_r/\nabla T_e$: ratios ≈ 1.8 and 1.7 follow from 4 data points for V_f and T_e outside of limiter shadows, averaged between the two probe pins (facing inner and outer divertors), for lower single-null (normal Bt direction) and upper single-null (reversed Bt direction) configurations, respectively. The reciprocating probe was introduced from the outer (low field) side just above the equatorial plane. Dimensionless collisionalities ν_{ee}^{*} calculated according to Eq. (1) were ≈ 16 and 12, for lower and upper single-null configurations, respectively, being similar to those for the modelled standard AUG Ohmic case. Data from the probe introduced from the inner (high field) side, however, were more complex, with E_r extracted from the first two probe positions (deepest in the plasma) being negative, but for positions further out – positive, with the $-eE_r/\nabla T_e$ ratio similar to those from the outside probe. Electron temperatures measured by the inside probe were substantially lower than those measured by the outside probe.

Low E_r values following from the code results presented here are a typical feature of solutions where neutrals are described by kinetic Monte-Carlo codes (Eirene and Nimbus in SOLPS and EDGE2D, respectively). In contrast, SOLPS cases with fluid neutrals exhibit higher E_r values and positive throughout most of the SOL, but with the $-eE_r/\nabla T_e$ ratios still well below 1 for the standard AUG Ohmic case. Examples of SOLPS solutions with fluid neutrals and positive E_r in the SOL can be found in [10] and [24]. The difference between cases with fluid and Monte-Carlo neutrals may be related to a much higher energy of neutrals in fluid cases, resulting in 'hot' (with high T_e) solutions in the divertor. However, as was pointed out earlier, even substantial variation of neutrals' behaviour in Eirene has not led to sufficiently 'hot' divertor solutions, that would be consistent with experiment. An issue of Monte-Carlo versus fluid neutral models and their impact on SOLPS solutions and E_r values will be thoroughly dealt with in the near future.

The present assumption is that the discrepancies between experimental and simulated E_r values should be attributed to the effect of supra-thermal electrons originating from the main SOL, upstream of the divertor. (No direct link between the $-eE_r/\nabla T_e$ ratios and collisionalities ν_{ee}^{*} can however be established from the analysis of experimental data presented here, although such a link is clearly seen in the SOLPS cases for the same magnetic configuration (lower density cases have larger $-eE_r/\nabla T_e$)). Unfortunately, to our knowledge, there is no direct experimental evidence confirming the existence of a significant population of energetic

electrons. Indirectly, in a number of publications (see e.g. [25] and refs. therein) it has been concluded that in medium density plasmas target probes read considerably higher T_e than the true local value due to the contribution of weakly collisional electrons originating in regions of higher temperatures further upstream.

So far, the strongest evidence for the existence of large population of supra-thermal electrons comes from kinetic modelling. In [5], a situation with a much higher upstream than downstream T_e and the ratio of Coulomb collisional mean-free path λ to the parallel plasma parameter variation scale length L of 0.1 (at the 'hot' end) was modelled with the Fokker-Planck kinetic code ALLA. Near the 'cold' boundary the electron heat flux was found to be totally dominated by tail electrons coming from hotter regions upstream, with the heat flux density being relatively constant (varying by not more than ≈ 50%) in the E_e/T_e range (E_e - electron kinetic energy) from 3 to 15, with T_e being local ('cold') electron temperature. At the same time, the 'hot' boundary was under-populated by hot electrons. This situation is very similar to that encountered in typical AUG plasmas [2] and also expected in ITER [5,2], with T_e varying strongly along the field lines and similar upstream collisionality levels. For example, for the SOLPS case simulating the second, higher density phase of the standard Ohmic AUG shot analysed in [2] and discussed in Sec. 2, the effective separatrix collisionality ν^*_{ee} at the outer midplane position determined according to Eq. (1) is equal to 14.1. This value is not far from the L/λ ratio of 10 used in the kinetic modelling, to which it can be directly compared. Since ν^*_{ee} reflects the collisionality of thermal electrons, supra-thermal electrons from the ~ 4th tail of the Maxwellian distribution (in velocity space) will have the effective L/λ ratio of ~ 0.1, for the nominal (that is, calculated for thermal speeds) L/λ ratio of 10, owing to the particle velocity scaling for the collisionality $\propto v_e^{-4}$. Hence, heat-carrying electrons in the SOL are usually very weekly collisional, and the use Braginskii's equation for the parallel electron heat flux is totally unjustified. Over-population of the 'cold' boundary by supra-thermal electrons may require introduction of 'flux enhancement factors' for the parallel electron heat flux near the divertor target modelled in fluid codes, in addition to frequently used 'flux limits' for the upstream plasma, as was concluded in the kinetic simulations in [26].

Very low E_r values obtained in the code simulations presented in this paper may raise questions of whether all the controlling physics influencing the distribution of electric potential in the SOL has been properly incorporated into the code(s). Effects of very long connection lengths in the SOL rings next to the separatrix (45 m from outer midplane to the target for AUG, on the first SOL ring), the influence of the private region on the adjacent SOL rings, influence of neutrals on the E_r distributions, non-ambipolarity of perpendicular/radial plasma transport due to drifts, poloidal asymmetries of plasma potential distributions, will be subject to detailed analysis in the future. Cases will also be run on a much finer mesh (although first tests made on a SOLPS mesh with a doubled number of rings in the SOL did not result in any significant alterations of the solutions).

A separate issue, independent from the fluid modelling of the plasma edge, is the large E_r compared to T_e gradients, measured in the SOL by the probes. In AUG, JT-60U and TCV, $-eE_r/\nabla T_e$ ratios were ~ 3 (somewhat smaller in JT-60U, ≈ 2.4, but exceeding this value in TCV). Since the primary physical parameter measured by the probes is the floating potential, the value of $-eE_r/\nabla T_e$ ratio obtained from the probe data depends critically on the value of the sheath potential drop Eq. (3). Since $e(V_p - V_f)/T_e = 3$ was assumed, for flat SOL V_f profiles

as those in Figs. 3 (for 'r'-values) and 7, one naturally obtaines $-eE_r/\nabla T_e \sim 3$. Equation 3, at the same time, is rather sensitive to the secondary electron emission coefficient δ which can increase dramatically under conditions of high electron temperature and high power fluxes onto the probe surface, up to the value $\delta \sim 1$ when the probe can go into self-emission. From a very limited database of measured V_f and T_e profiles considered in this paper no correlation between the magnitude of T_e and $-eE_r/\nabla T_e$ ratios can however be established. This seems to suggest that the secondary electron emission didn't play a significant role in the measurements. However, it is known that secondary electron emission is very sensitive to surface conditions and topography, and reliable values of δ can be obtained only by a study of the material in the condition found in the particular experiment ([7], p.116). For a pure graphite surface (graphite was the material of the probe pins in all experiments described in this paper) and $T_e = 50$ eV, $\delta = 0.544$ follows from Eq. (3.5) and Table 3.1 of [7] (pp.115-116). This equation approximates very well the experimentally found normalized secondary electron emission coefficient given in Fig. 3.5 of this the same ref. Substituting this δ into Eq. (3) would give $e(V_p - V_f)/T_e = 2.55$. For $T_e = 100$ eV, $\delta = 0.777$ is obtained, giving $e(V_p - V_f)/T_e = 1.84$. This would be more in line with estimates made below in this section for high recycling divertor regimes. It has to be noted however, that a low energy electron released from a surface, when the magnetic field is rather oblique to the surface (which is typically the case in divertor configurations), has a finite Larmor radius and thus has a good chance of immediately returning to the surface within one Larmor period. The *effective* electron emission coefficient for fusion devices is thus sometimes taken to be zero, regardless of the original release rate ([7], p.114). Summarising, one has to conclude that the available data is insufficient to neither claim that the probe-invoked $-eE_r/\nabla T_e$ ratios were grossly overestimated by the neglect of higher secondary electron emission at positions closer to the separatrix, nor to expect that the effect of the secondary electron emission can be neglected. Its influence on the experimental results for the $-eE_r/\nabla T_e$ ratio remains an open question.

In contrast to the Langmuir probe data, E_r invoked from the Doppler reflectometry measurements on AUG, discussed in Section 2, combined with the T_e profile measured by the YAG laser would imply significantly smaller $-eE_r/\nabla T_e$ ratios, < 1. The cause of the difference between the two methods of evaluating these ratios is presently not understood. It has to be pointed out, however, that neither Langmuir probe nor Doppler reflectometer technique allows one to measure E_r directly. Evaluation of this quantity from the reflectometer data depends on the knowledge of the phase velocity of plasma density fluctuations. Its evaluation from Langmuir probe measurements depends on the theoretical relation between floating potential V_f measured by the probe and plasma potential V_p, as discussed above, and on the magnitude of measured T_e. Increased secondary electron emission in the 'near SOL' can reduce the discrepancy between the probe and reflectometer E_r values, but is unlikely to eliminate it completely.

Large $-eE_r/\nabla T_e$ ratios, of order 3, with T_e being the upstream electron temperature, measured near the outer midplane position, rather than target temperature, are inconsistent with simple estimates that can be obtained for high-recycling SOLs. In the SOL, radial electric field is determined mainly by parallel plasma transport and interaction with the target. The upstream plasma potential is related to the target potential via the Debye sheath and magnetic pre-sheath (MPS) drops at the target and the potential difference spread along the field line:

$$V_{p,upstream} = V_{p,target} + \Delta V_{Debye} + \int E_{\parallel} ds_{\parallel} , \qquad (4)$$

where ΔV_{Debye} is the potential drop near the target due to the Debye sheath and MPS, $E_{||}$ is the parallel electric field, and the integral is taken from the plasma position near the target, but outside of the MPS which is of width a few ion Larmor radii ([7], p.99), to the upstream position, e.g., near the outer midplane. The parallel electric field in turn can be expressed as:

$$E_{||} = -0.71\nabla_{||}T_e / e - \nabla_{||}p_e / en_e + j_{||} / \sigma_{||}, \quad (5)$$

following from the parallel electron force balance. The first term on the right hand side (RHS) of this equation describes the electron thermo-force; coefficient 0.71 is correct for singly charged ions, but is lower for higher charge states.

For the simplest SOL model with no neutral ionization, poloidally constant T_e and plasma potential V_p, no parallel currents etc., one expects small $E_{||}$ and $\Delta V_{Debye} \sim 3T_e/e$, yielding $-eE_r/\nabla T_e \sim 3$, which would be in agreement with some of the experiments showing similar $-eE_r/\nabla T_e$ ratios. In most of the experiments, however, strong recycling in the divertor results in a much lower target than upstream T_e. Negative parallel current density (driven by electrons) directed towards the outer target from the inner, provided the outer target is hotter (which is the most typical case), reduces upstream potential due to the contribution from the $j_{||}/\sigma_{||}$ term. It however also reduces the target sheath drop ΔV_{Debye}, and these two effects partly cancel each other out. In the absence of plasma-neutral interactions and cross-field drifts (an idealistic case), the plasma pressure drops by ~ factor 2 towards the target, an effect compensated by the plasma acceleration towards the target up to the ion sound speed (thus, contributing to the 'kinetic pressure'). This raises the plasma potential upstream with respect to the target potential due to the contribution of the $-\nabla p_e/en_e$ term. Interaction with neutrals can lead to more substantial pressure drop, resulting in the *detachment* of the plasma from the target (see e.g. [27]). The influence of neutral ionization and charge-exchange processes on the upstream E_r profile via radial variation of the $-\nabla p_e/en_e$ term contributions (parallel gradient implied) is presently being assessed in dedicated EDGE2D code runs. The estimate given below which takes into account only the sheath drop $\Delta V_{Debye} \sim 3T_e/e$ and electron thermo-force and ignores the $-\nabla p_e/en_e$ term, gives a rough estimate for the radial electric field provided there is no strong non-ambipolarity of the radial plasma transport:

$$eE_r \sim -3\nabla T_{e,target} - 0.71\nabla(T_e - T_{e,target}), \quad (6)$$

where the gradient is taken upstream of the target along the radial direction, and target T_e values are projected along field lines upstream. For the case of $T_{e,target}$ equal to the upstream electron temperature, this formula predicts $-eE_r/\nabla T_e \sim 3$, as pointed out above. For realistic cases with lower target temperatures, e.g. being only ~ ½ of the upstream ones, one obtains: $-eE_r/\nabla T_e \sim 1.85$. Ratios $-eE_r/\nabla T_e \sim 1.5$ following from some experiments (JET, Alcator C-Mod) may therefore be considered as not being in a strong disagreement with simple estimates. At the same time, $-eE_r/\nabla T_e$ ratios ~ 3 cannot be explained unless one assumes strong non-ambipolarity of the radial plasma transport or that the potential drop near the target is $> 3T_{e,target}/e$. The latter would be in line with the leading assumption about the cause of the discrepancies between simulated and experimental T_e at the target and E_r in the SOL, relating both to the presence of a significant fraction of supra-thermal electrons at the target. It is probable that these, energetic electrons can contribute not only to the target heat flux but also to the Debye sheath formation. This would require electrons from upstream with velocities in the 3-5 v_{T_e} range, responsible for the bulk of the parallel heat flux, to cascade

down the energy scale via collisions with slower electrons on their way to the target, and to contribute significantly to the energy spectrum around $3T_{e,target}$, responsible for the formation of the sheath. However, the notion of 'electron temperature' with respect to the near target electron component may then be ill defined, as the electron energy distribution may be far from Maxwellian.

7. Summary

The E_r profiles in the SOL simulated with the two widely used edge codes – SOLPS and EDGE2D, are in a disagreement with experimental data obtained in ASDEX Upgrade (AUG) and JET. They also contradict the supporting experimental evidence obtained with reciprocating Langmuir probes on JT-60U and TCV. Experimental profiles exhibit a positive E_r throughout the SOL, with the plasma electric potential V_p falling together with electron temperature T_e, and with the ratio $-eE_r/\nabla T_e$ varying between 1.6 and 5. In contrast, in the modelling with Monte-Carlo neutrals, V_p profiles are found to be fairly flat in most of the SOL. For the same magnetic configuration and input power levels, the simulated E_r rises with the decrease in the separatrix density. Nevertheless, reducing density in the simulations didn't produce large enough E_r values relative to $-\nabla T_e/e$ that would be consistent with the experiment. Further modelling will be performed with both fluid and Monte-Carlo neutrals in order to understand the origin of a difference between these cases and to check whether all the controlling physics influencing the V_p distribution in the SOL has been included and/or correctly implemented in the codes.

In contrast to large $-eE_r/\nabla T_e$ ratios following from Langmuir probe measurements, Doppler reflectometer measurements in the standard Ohmic regime of AUG seem to indicate low values of this ratio in the SOL, assuming the phase velocity of density fluctuations measured by the reflectometer is approximately zero. There is, on the other hand, no direct conflict between E_r values coming from the reflectometer and Langmuir probe data. Measured E_r values are similar, but the probe position was further away from the separatrix.

Discrepancies between probe measured and code simulated $-eE_r/\nabla T_e$ ratios are consistent with the recently made conclusion, based on the benchmarking of the SOLPS code against the AUG experiment, that fluid codes tend to underestimate T_e in the divertor. This is likely to be explained by the presence of supra-thermal electrons originating from the upstream (e.g. midplane), which are usually only weakly collisional and cannot be described by fluid codes. The final answer will only become available after incorporation of kinetic effects into the present-day fluid codes enabling one to switch these effects on and off in the code runs simulating well-diagnosed experimental plasmas.

It is at present not clear whether the extra parallel electron power flux to the divertor carried by energetic electrons and the consequent rise in the target T_e, can be solely responsible for the discrepancies in $-eE_r/\nabla T_e$ ratios, via the mechanism of Debye sheath and magnetic pre-sheath formation, with the potential drop being ~ $3T_e/e$ at the target. It is also possible that a large fraction of supra-thermal electrons from the upstream cascade down the energy scale on their approach to the target, increasing the potential drops at the target, thereby providing an extra increase of E_r in the SOL. Under such conditions the correct evaluation of T_e from Langmuir probes may become problematic due to strong deviations of the electron distribution function from Maxwellian. Experimental evidence from AUG, JT-60U and TCV, where $-eE_r/\nabla T_e$ ratios of order 2.5 and above (up to 5) were observed, indicate the possibility

of energetic electrons directly influencing the target Debye sheath. It is also possible, however, that the probe-invoked E_r values can be overestimated due to the assumption $e(V_p - V_f)/T_e = 3$ used for deriving radial electric field from T_e and V_f measurements. The difference $(V_p - V_f)$ is sensitive to the adopted secondary electron emission coefficient δ. The ratio $e(V_p - V_f)/T_e = 3$ corresponds to the adopted value of $\delta = 0.3$. In reality, δ can be lower or higher than 0.3 depending on the local electron temperature and the probe surface conditions. Under all circumstances, however, δ is expected to rise with the increase in T_e. Due to the uncertainty in the values of δ, it is at present not possible to estimate the extent of a possible downward correction for the $-eE_r/\nabla T_e$ ratios caused by secondary electron emission.

A large underestimate of E_r in the SOL by the present-day edge fluid codes is related with another known problem: the codes consistently underestimate parallel ion flows in the SOL measured with double-sided Langmuir probes ('Mach probes'). In the experiment, the radial electric field, together with the ion pressure gradient, is found to be one of the drivers for the part of the parallel ion flow which is dependent on the direction of the toroidal magnetic field, under the assumption that the ion Pfirsch-Schlüter flow is the major contributor to the measured ion flow [21,22,28]. An underestimate of E_r in the codes therefore directly contributes to the discrepancy between simulated and experimental parallel ion flows. According to estimates, the inclusion of correct, experimental E_r values in the theoretical formulas for the parallel ion Mach number can completely eliminate the difference between field-dependent parts of simulated and experimental flows in JET and significantly reduce the flows discrepancy in the AUG case [9].

References

[1] Chankin A V, Coster D P, Dux R, et al., Plasma Phys. Control. Fusion 48 (2006) 1839.

[2] Chankin A V, Coster D P, Dux R, et al., 'Comparison between measured divertor parameters in ASDEX Upgrade and SOLPS code solutions', paper P1-40 presented at the 17th PSI Conference, Hefei, May 22-26 (2006), accepted for publication in J. Nucl. Mater.

[3] Chankin A V, Coster D P, Dux R, et al, 'Critical issues identified by the comparison between experimental and SOLPS modelling on ASDEX Upgrade', in *Proc. of the 21st IAEA Conference, Fusion Energy, Chengdu, China, October 16-21 2006, (CD-ROM),* paper IAEA-CN-149/TH/P6-15, Vienna, 2006, IAEA.

[4] Braginskii S I, *Review of Plasma Physics* (Consultants Bureau, New York, 1965), Vol. 1, p. 205.

[5] Batishchev O V, Krasheninnikov S I, Catto Peter J, et al., Phys. Plasmas 4 (1997) 1672.

[6] Chodura R, Contrib. Plasma Phys. 28 (1998) 4/5, 303.

[7] Stangeby P C, in *The Boundary of Magnetic Fusion Devices*, IOP Publishing, Bristol (2000).

[8] Coster D P, Bonnin X, Chankin A, et al., 'Integrated modelling of material migration and target plate power handling at JET', in *Proc. of the 20th IAEA Conference, Fusion Energy, Vilamoura, Portugal, November 1-6 2004, Chengdu, China, October 16-21 2006, (CD-ROM),* paper IAEA-CN-116/TH/P5-18, Vienna, 2006, IAEA.

[9] Chankin A V, Coster D P, Asakura N., et al., 'The Role of Radial Electric Field in Driving Parallel Ion Flow in the Scrape-off Layer of Divertor Tokamaks', submitted for publication in Nuclear Fusion.

[10] Coster D P, Chankin A V, Conway G D, et al., proc. of 32nd EPS Conference on Plasma Phys. Tarragona, 27 June – 1 July 2005 ECA Vol.29C, P-1.008 (2005).

[11] Kukushkin A S, Pacher H D, Pacher G W, Janeschitz G, Coster D, Loarte A and Reiter D, Nucl. Fusion 43 (2003) 716.
[12] Erents S K, Pitts R A , Fundamenski W , Gunn J P and Matthews G F, Plasma Phys. Control. Fusion 46 (2004) 1757.
[13] Erents S K, Fundamenski W, Corrigan G, Matthews G F, Zagorski R, 'EDGE2D modelling of JET and ITER Including the Combined Effect of Guiding Centre Drifts and an Edge Transport Barrier', paper P3-6 presented at the 17th PSI Conference, Hefei, May 22-26 (2006), accepted for publication in J. Nucl. Mater.
[14] Müller H.W., Bobkov V., Rohde V., et al., proc. of 32nd EPS Conference on Plasma Phys. Tarragona, 27 June – 1 July 2005 ECA Vol.29C, P-1.009 (2005).
[15] Müller H.W., Bobkov V., Herrmann A., et al., 'Deuterium plasma flow in the scrape-off layer of ASDEX Upgrade', paper P3-15 presented at the 17th PSI Conference, Hefei, May 22-26 (2006), accepted for publication in J. Nucl. Mater.
[16] Conway G, Schirmer J, Klenge S, Suttrop W, Holzhauer E and the ASDEX Upgrade Team, Plasma Phys. Control Fusion 46 (2004) 951.
[17] Scott B D, private communication (2006).
[18] Conway G, Schirmer J, Angioni C, et al., 'Study of Turbulence and Radial Electric Field Transitions in ASDEX Upgrade using Doppler Reflectometry', in *Proc. of the 21st IAEA Conference, Fusion Energy, Chengdu, China, October 16-21 2006, (CD-ROM),* paper IAEA-CN-149/EX/2-1, Vienna, 2006, IAEA.
[19] Dong J Q, Horton W, and Kim J Y, Phys. Fluids B4 (1992) 1867.
[20] Stangeby P C, Phys. Fluids 27 (1984) 682.
[21] Asakura N, Sakurai S, Shimada M, Koide Y, Hosogane N, and Itami K, Phys. Rev. Lett. 84 (2000) 3093.
[22] Pitts R A, Horacek J, Wischmeier M, 'Parallel SOL flow in TCV', paper O-16 presented at the 17th PSI Conference, Hefei, May 22-26 (2006), accepted for publication in J. Nucl. Mater.
[23] LaBombard B, Rice J E, Hubbard A E, et al., Nucl. Fusion 33 (2004) 1047.
[24] Rozhansky V, Kaveeva E, Voskoboynikov S, et al., Plasma Phys. Control. Fusion 48 (2006) 1425.
[25] Horacek J, Pitts R A, Stangeby P C, Batishchev O, Loarte A, J. Nucl. Mater 313-316 (2003) 931.
[26] Kukushkin A S, Runov A M, Contrib. Plasma Phys. 34 (1994) 2/3, 204.
[27] Loarte A, Monk R D, Martín-Solís J R, et al., Nucl. Fusion 38 (1998) 331.
[28] Asakura N, and ITPA SOL and divertor topical group, 'Understanding the SOL flow in L-mode Plasma on divertor tokamaks, and its influence on the plasma transport', paper R-5 presented at the 17th PSI Conference, Hefei, May 22-26 (2006), accepted for publication in J. Nucl. Mater.